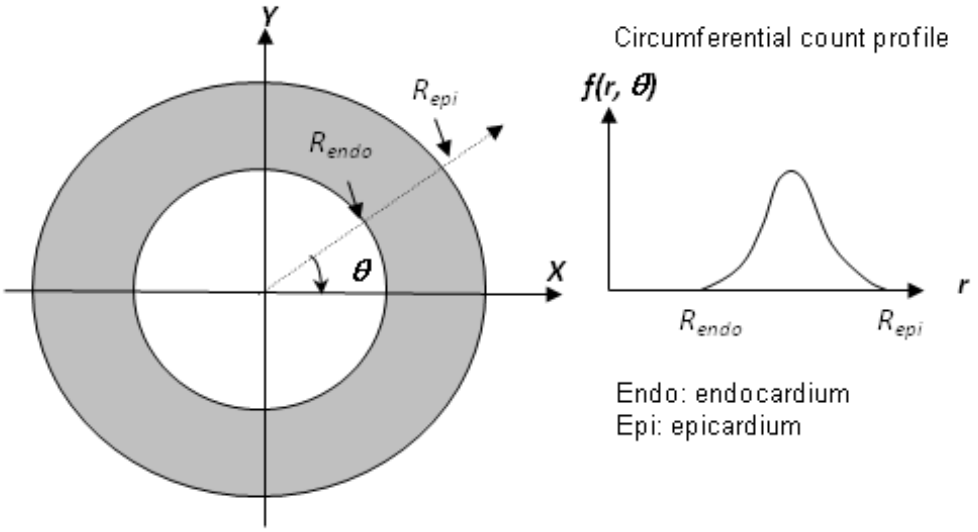

SUPPLEMENTAL FIGURE 1. Schematics of myocardial segment and the corresponding circumferential count profile for the detection of contaminated myocardial segments by extracardiac activity.

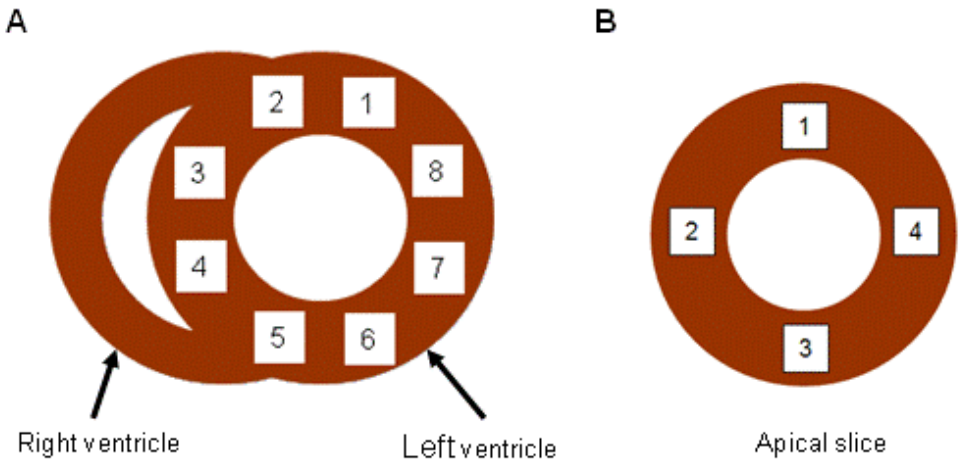

SUPPLEMENTAL FIGURE 2. Schematics of the numbering sequence used for identification of the various myocardial segments of the core LV myocardium (A) and the apex (B).

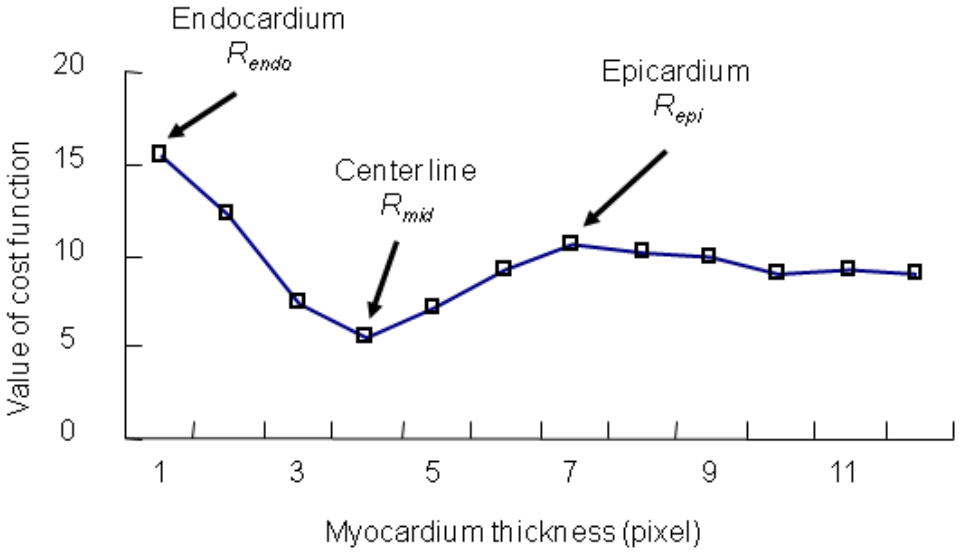

SUPPLEMENTAL FIGURE 3. Demonstration of the cost function for estimation of LV myocardial thickness.

SUPPLEMENTAL APPENDIX

Left Ventricular Cavity Separation from CT

After administration of a contrast agent for CT imaging, image intensity in the LV blood pool is relatively higher than that in the myocardium. The separation of the LV cavity is achieved via the level-set framework (*13*). The idea of level set method is evolving a surface ϕ instead of a front defined implicitly as the zero level set $\phi = 0$. A point x belonging to a front evolves over time so that $x(t)$ is its position in 3-D coordinate over time. At any time t (i.e. iteration number), for each point $x(t)$ on the front the surface has the height of 0 by definition, i.e. $\Gamma(t) = \{x \mid \phi(x(t), t) = 0\}$. The initial ϕ can actually be any arbitrary functions as long as its zero level set matches the initial contour, and in our case it is defined by the seed region being put in the cavity of the LV. The surface height (ϕ) is equal to the distance from $x(t)$ to the closest point on the front $\Gamma(t)$, in which the distance is defined as positive when $x(t)$ is outside the contour, and as negative otherwise. Given an initial ϕ at $t = 0$, it is possible to identify ϕ at any time t with the motion equation ($\frac{d\phi(x(t),t)}{dt} = 0$). Using the chain rule, we have

$$\frac{\partial \phi(x(t),t)}{\partial t} + F\left|\nabla \phi(x(t),t)\right| = 0 . \qquad \text{Supplemental Eq. 1}$$

Let I denote an *in vivo* CT image. The speed term F used in Supplemental Eq. 1 above can be formulated as (*1*)

$$F = \alpha \cdot g_I - \beta \cdot \kappa \cdot g_I - \gamma \frac{\nabla g_I \cdot \nabla \varphi}{\left|\nabla \varphi\right|}, \qquad \text{Supplemental Eq. 2}$$

where $g_I = \frac{1}{1+\left|\nabla(G_\sigma * I)\right|}$ and $\kappa = \nabla \cdot \frac{\nabla \phi}{|\nabla \phi|}$. The expression $G_\sigma * I$ denotes the *in vivo* CT image convolved with a Gaussian smoothing filter of which the characteristic width is denoted as σ.

The Gaussian filter is used to smooth the noise in the LV edges and to facilitate edge detection for the anatomical structures of the LV. There are three terms involved in this level-set algorithm. The first term in Supplemental Eq. 2 is a constant speed and the second term is for a curvature-based geometric smoothing in which κ is the curvature. The last term $\frac{\nabla g_I \cdot \nabla \phi}{|\nabla \phi|}$ in Supplemental Eq. 2 is used to direct the curve to the middle of the LV cavity boundary. Scalars α, β and γ are the parameters used to weigh the relative influence of each of the terms on the movement of the edges. The parameters α, β and γ determining the LV cavity separation can be defined by running a number of tests with different values of α, β and γ. In this study, α, β and γ were determined empirically as 0.5, 0.5 and 5, respectively.

A proper initialization is critical for the level-set algorithm. A seed region with one or more pixels needs to be manually introduced into the cavity volume. Ultimately, the cavity volume is updated iteratively with the speed term F until it reaches the endocardial edges.

Left Ventricular Epicardial Edge Detection from CT

Our detection of the epicardial edge is incorporated with the prior information of LV myocardial thickness (~ 2 mm for rats). In this animal study, we assumed initially a constant thickness for the entire LV myocardium and the epicardial edge in the CT volumetric images was estimated based on the maximal gradient magnitude of image intensities and the equal LV thickness surface. The edge map of the *in vivo* CT is derived from $\nabla(G_\sigma * I)$, where I is the CT image and G_σ is a Gaussian smoothing filter. In order to suppress non-maximal pixels in the edge map obtained above and refine the edge ridges, the sign of the third derivative of the CT images is used to finalize the local extrema (*2*). The epicardial edge map *(D)* in our

algorithm is defined as

$$D = \begin{cases} \nabla(G_\sigma * I), & \nabla^3(G_\sigma * I) \le 0 \\ 0, & \nabla^3(G_\sigma * I) > 0 \end{cases}. \qquad \text{Supplemental Eq. 3}$$

As seen, the edge map is not changed if the sign of the third derivative is less than 0 and is set to 0, otherwise. The signed distance map is generated with the incorporation of the LV cavity volume obtained from the CT segmentation. In the signed distance map, pixel values represent the shortest signed distance of the points from the edge of LV cavity (endocardium). The cost function is designed to provide the local maximum response between the distance 0 (endocardial edge, R_{endo}) and the distance from the edge of the LV cavity (epicardial edge, R_{epi}). The endocardial edge (R_{endo}) is derived from the CT image segmentation of the LV cavity and the distance from R_{endo} ($w = 0$) to the "mid-wall" of the LV myocardium (R_{mid}) is determined by

$$R_{mid} = \arg\min_{w} \left(\iint_{Sw} d_w \Big/ sum_w \right), \quad w \in (0, R_{\max}), \qquad \text{Supplemental Eq. 4}$$

where d_w represents voxel value on the isosurface defining the edge map D (see Supplemental Eq. 3), Sw denotes a set of the isosurfaces, sum_w is the number of voxels on the isosurface within Sw, and R_{max} is a predefined search limit chosen as the width of 12 pixels used in this study. Consequently, the width of the LV myocardium (W) can be estimated by

$$W = \arg\max_{w} \left(\iint_{Sw} d_w \Big/ sum_w \right), \quad w \in (R_{mid}, R_{\max}) \qquad \text{Supplemental Eq. 5}$$

and the myocardial volume V_{LV} can be obtained by integrating all the voxels within the

myocardial thickness W estimated above.

Supplemental References

<jrn>1. Caselles V, Kimmel R, Sapiro G. Geodesic active contours. *Int J Comput Vis*. 1997;22:61–79.</jrn>

<jrn>2. Canny J. A computational approach to edge detection. *IEEE Trans Pattern Anal Mach Intell*. 1986;8:679–698. PubMed</jrn>